

# Pulsed Fiber Laser “SumiLas<sup>\*1</sup>” for Micro-Processing

Motoki KAKUI\*, Shinobu TAMAOKI, Yasuomi KANEUCHI, Hiroshi KOHDA, Yuji TANAKA, Yasuhiro OKAMOTO, Yoshiyuki UNO and Brian BAIRD

In order to meet requirements in the next generation micro-processing, we have developed a 1.06 $\mu\text{m}$  pulsed fiber laser employing a MOPA (master oscillator power amplifier) configuration. This laser features broad pulse width flexibility (100ps to 20ns), excellent beam quality ( $M^2 \leq 1.3$ ), and a wide range of pulse repetition frequencies (50kHz to 1MHz). With these attributes of the laser, the optimum pulse width for P1 processing both (a)-Si (amorphous silicon) and CIS or CuInSe (copper indium diselenide) types of solar cells was studied. As a result, it was found that the pulse width of 10 to 20ns gives the best scribing quality on (a)-Si solar cells while the pulse width around 500ps leads to excellent results for CIS samples. The scanning speeds of 2500mm/s and 5000mm/s have been achieved for (a)-Si and CIS samples, respectively. In this study, surface texturing of STAVAX, a through-hardening stainless steel for plastic molding, was also conducted. The surface roughness and water repellency on the STAVAX surface were controlled by adjusting the pulse width, number of scanning and assist gas condition.

Keywords: laser, pulse, micro-processing, solar cell, texturing

## 1. Introduction

Recently, laser processing has been replacing some conventional mechanical or chemical processing in various industries because of the following advantages<sup>(1)</sup>:

- non-contact processing,
- focus control and flexible positioning by optical guidance, and
- reduction of environmental impact.

In micro-processing of electronic components, pulsed lasers have become particularly important due to the trend in downsized components and diversification of materials.

Despite the widespread use in the various industries, the ablation phenomena caused by the laser pulse has not yet been fully elucidated because the phenomena involve various effects such as plasma generation, evaporation, melting and shock waves as shown in Fig. 1<sup>(2)</sup>. To avoid the

thermal effects that lead to dross and debris, it has been believed that the pulse must be shortened. As shown in Fig. 2, however, a pulse width shorter than 100fs tends to degrade the processing quality because of its nonlinear effects. Therefore, a pulse width ranging from 1ps to 100ps is considered most appropriate for micro-processing<sup>(3)</sup>.

Q-switching<sup>\*2</sup> and mode-locking<sup>\*3</sup> methods have been well known for pulse generation<sup>(4)</sup>. In general, the latter method is used to generate the pico-second (ps) optical pulse<sup>(5)-(7)</sup>. However, due to its instability and high operational cost, the mode-locked ps laser has not become the mainstream. Therefore, the Q-switching laser, which is comparatively inexpensive, is widely used in today's market despite the pulse width range of several tens to hundreds nano-seconds (ns), which results in the thermal effects in laser processing. Recently, MOPA<sup>\*4</sup> type lasers have been attracting attention because of the excellent capability of controlling the temporal pulse shapes. However, most of the MOPA lasers now in use have the pulse width tuning

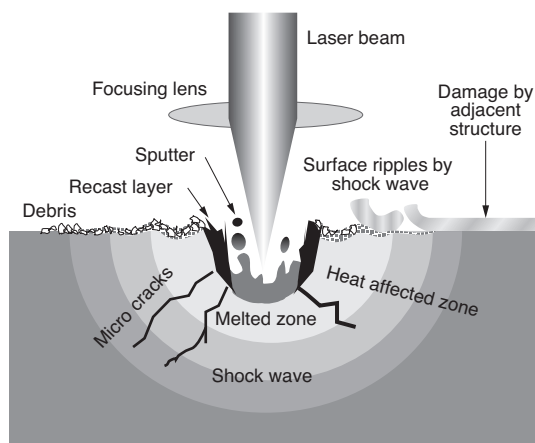


Fig. 1. Various effects accompanying laser ablation<sup>(2)</sup>

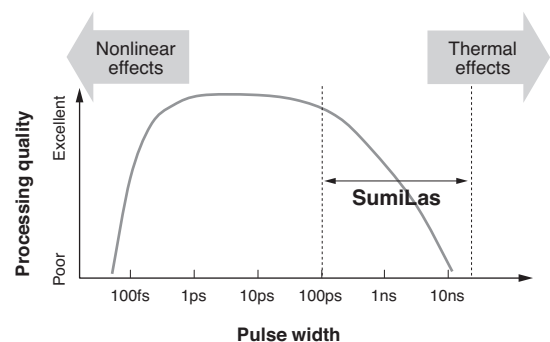
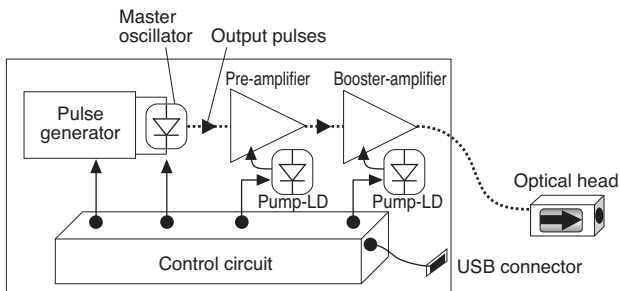


Fig. 2. Relationship between processing quality and pulse width<sup>(3)</sup>  
SumiLas can cover the range between the broken lines.

range of around 10ns to several hundreds ns, where thermal effects often negatively affect processing quality<sup>(8),(9)</sup>.

To address the problem, we have developed a MOPA-type pulsed fiber laser “SumiLas” by utilizing optical fiber communication technology such as high-speed pulse modulation and low-noise and high-gain optical amplification. SumiLas has a variable pulse width range from 100ps to 20ns, and its configuration is relatively simple as shown in **Fig. 3**. Thus, SumiLas enables high processing quality at the same level of almost as excellent as the mode-locked ps lasers<sup>(6),(7)</sup> and at a comparable price to the Q-switching lasers.



**Fig. 3.** Schematic diagram of SumiLas

This paper presents examples of micro-processing using SumiLas: P1 structuring on the two types of thin-film solar cells, namely amorphous (a)-Si and CIS<sup>\*5(10)</sup>; and surface texturing of stainless steel<sup>(11),(12)</sup>. In both cases of a-Si and CIS cells, excellent processing quality has been demonstrated. While the result of P1 structuring to a CIS cell was equivalent to that obtained by ps-lasers<sup>(6),(7)</sup>, it was revealed that conventional ns-pulses were more suitable for a-Si cell processing.

This paper also reports on the second harmonic generation of SumiLas, which is an important factor to realize P2 and P3 structuring on solar cells.

## 2. Performances of SumiLas

**Figure 4 (a)** shows a photograph of SumiLas. The dimensions (in mm) of the SumiLas are 500 (depth) x 482 (width) x 200 (height). It contains a specially designed pulse generator to directly modulate the seed laser diode oscillating at 1060nm. Its repetition rate is normally tuned in the range from 50k to 1MHz. Output pulses are amplified by optical amplifiers which employ Yb-doped fiber, and the average output power available is 15W. An optical head box containing a collimator and isolator is usually attached at the end of the delivery fiber. The output beam diameter is set to about 1.0mm. The beam quality is excellent as shown in **Fig. 4 (b)**, and typical  $M^2$ \*6 is less than 1.1.

**Figures 5** show the examples of the pulse shapes (a) when the electric pulse width is set to 20 ns in the standard

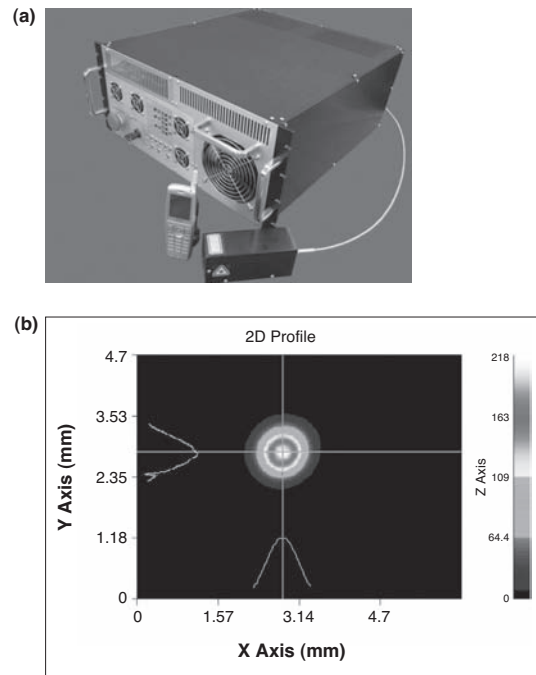


**Fig. 4.** (a) Appearance of SumiLas and (b) example of output beam profile

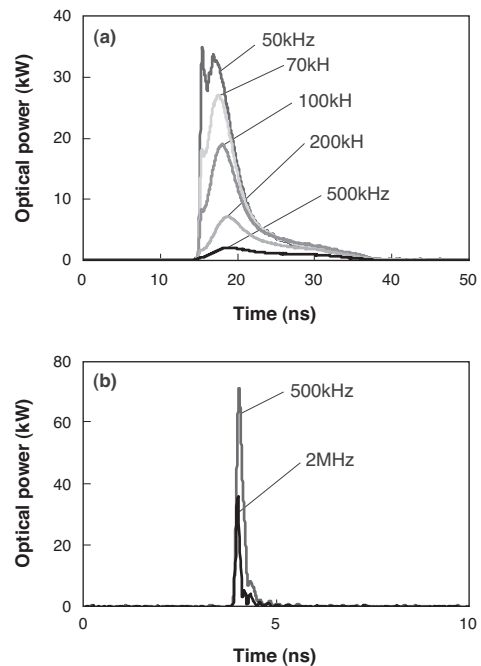


**Fig. 5.** Examples of output pulse shapes under (a) standard mode and (b) short pulse mode

mode, and (b) when the short pulse mode is adopted. As shown in **Fig. 5 (a)**, the FWHM (full width of the half maximum) of the optical pulses decreases as the repetition rate becomes lower, mainly because of the transient response of the fiber amplifiers, while the width of the pulse base always coincides with the electric pulse width, namely 20ns

in this case. In the short pulse mode, the FWHM is in the range of 100 to 200ps, and the width of the pulse base is always shorter than 1ns.

### 3. P1 Structuring on Solar Cells<sup>(10)</sup>

Today, crystalline Si-type solar cells are most popularly used all over the world. In order to achieve the grid parity, however, active R&D of the novel configuration is under progress. A thin-film type solar cell structured on a glass panel is considered to be one of the most promising candidates. In the fabrication process, P1 to P3 structuring, as shown in **Fig. 6**, needs to be performed. In almost all types of thin-film solar cells, P1 structuring can be done at the wavelength of 1060nm, while P2 and P3 structuring requires the laser oscillating at 530nm. The area between P1 and P3 scribing lines is called a “dead zone” because this area does not contribute to the power conversion, and needs to be reduced in the future. Moreover, the laser scanning speeds for P1 structuring need to be increased to higher than the current value of around 1000 to 1500mm/s in order to reduce the fabrication cost. To meet these requirements simultaneously, MOPA type fiber lasers featuring the diffraction-limited beam and the high repetition rate is expected to be a suitable solution. It should be noted that the processing quality is also important from the viewpoint of the reliability because solar cells must work for longer than 25 years after the installation.

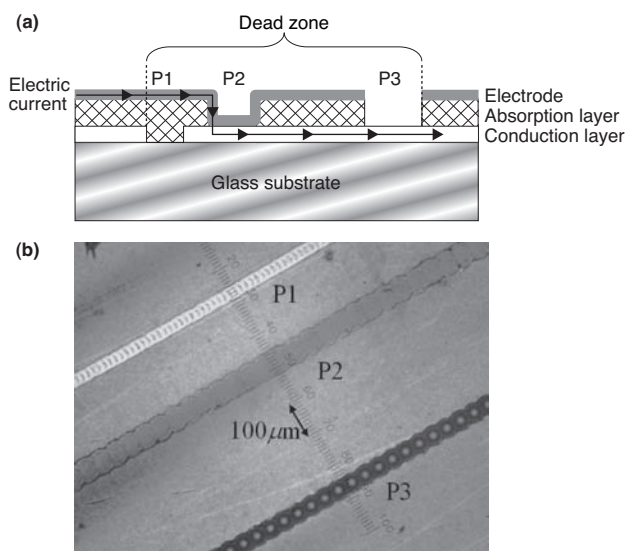


**Fig. 6.** (a) Cross section of P1, P2 and P3 structures on thin-film solar cell, and (b) Photograph of the sample by American major manufacturer

To demonstrate the advantage of SumiLas, we have tried P1 scribe tests on two types of the PV materials, namely

- (1) NFL310SA2 made by Nippon Sheet Glass Co., Ltd.
- (2) MOLY made by AGC solar Belgium

Sample (1) is utilized for a-Si type or CdTe type solar cells, and the coating on it is mainly composed of SnO<sub>2</sub>. Sample (2) with Mo coating is used for CIS (CuInSe) type solar cells. Substrate for both samples comprises soda-lime glass.

The output beam diameter has been set to 1.0mm. A beam expander was inserted after the optical head box to magnify the beam diameter 5 times. The galvano scanner “Scanlab Hurryscan II-14” and the f-theta lens “Scanlab ID 114286” with the focusing length of 100mm have been employed instead of a high-speed linear stage. The laser beam is radiated on the glass-side of the samples. The beam spot diameter on the coating surface has been calculated to be 34μm.

Both the standard mode and short-pulse mode shown in **Fig. 5 (a) and (b)**, respectively, have been tried for this experiment. The average power and the repetition rate have been optimized to achieve the target scanning speed of 2500mm/s for Sample (1), and 5000mm/s for Sample (2). The optimized conditions are shown in **Table 1**, and the P1 structuring results are shown in **Fig. 7, Photo 1, 2, and Fig. 8**. **Figure 7** shows the inspection result of P1 structuring on Sample (1) with 20ns pulse with the optical microscope and SEM<sup>\*7</sup>. There has been no damage, such as micro-crack, either on glass or on TCO coating.

**Table 1.** Conditions of P1 structuring on Samples (1) and (2)

| Sample | Pulse width (ns) | Average power (W) | Repetition rate (kHz) | Scanning speed (mm/s) |
|--------|------------------|-------------------|-----------------------|-----------------------|
| ①      | 20               | 10                | 160                   | 2500                  |
|        | 0.2              | 6.8               | 150                   | 2000                  |
| ②      | 20               | 8                 | 250                   | 5000                  |
|        | 0.5              | 5.7               | 250                   | 5000                  |

According to the composition analysis results by EDX<sup>\*8</sup>, there is no residual of SnO<sub>2</sub> on the glass substrate. Therefore, the isolation resistance is higher than 100MΩ. Moreover, the 3-D analysis result by New View<sup>\*9</sup> 200 manufactured by Zygo shows no sign of the debris or lift off. The thickness of the TCO film in Sample (1) is 640nm as shown in **Fig. 7 (d)**.

On the other hand, when 200ps-pulses are employed for P1 structuring on Sample (1), each spot size remarkably shrinks, and moreover, significant cracks and foams can be observed on the glass substrate although the average power on the work piece has been set to only 6.8W as shown in **Photo 1**. The excessively high peak power shown in **Fig. 5 (b)** seems the cause of the damage to the glass. The hypothesis “the shorter pulse is the better” is apparently not valid in the case of Sample (1).

On the other hand, 20ns-pulses cause the significant thermal effects, namely cracks, wrinkles around each spot, and rolling up between spots as shown in **Photo 2**. In the experiment employing the short-pulse mode, the pulse width has been slightly widened up to 500ps so as to avoid

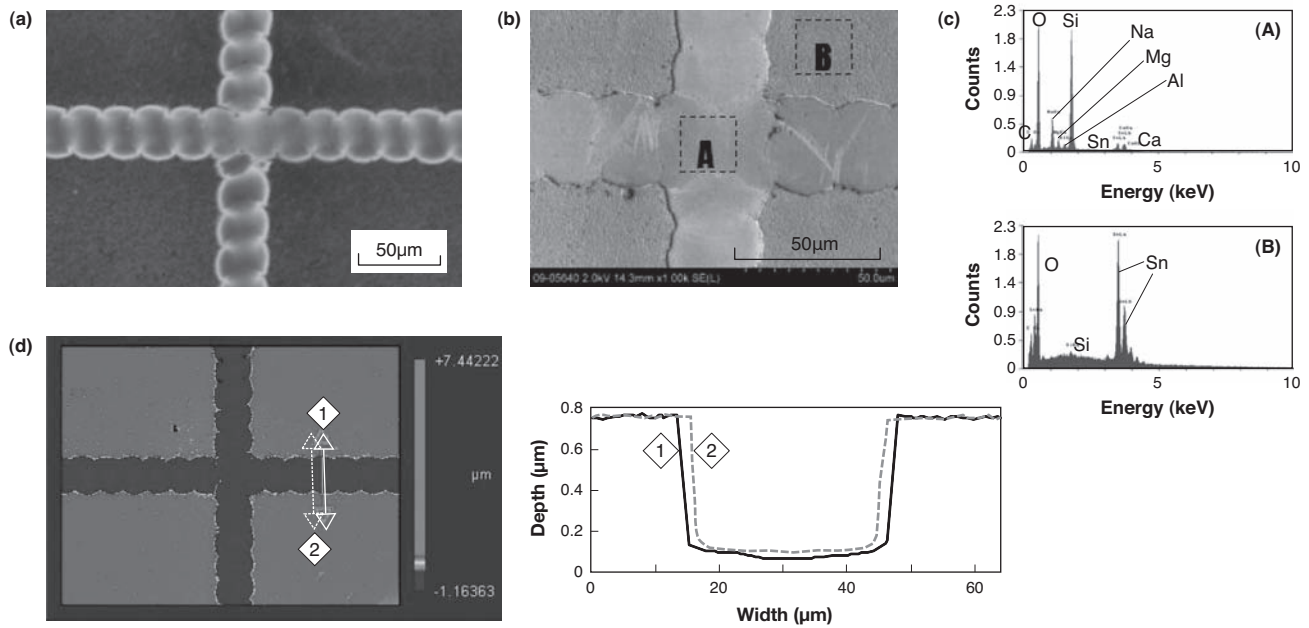


**Fig. 7.** P1 structuring on Sample (1) with 20ns-pulses observed with (a) optical micro-scope, (b) SEM, (c) EDX, and (d) 3-D analysis with microscope-based interferometer

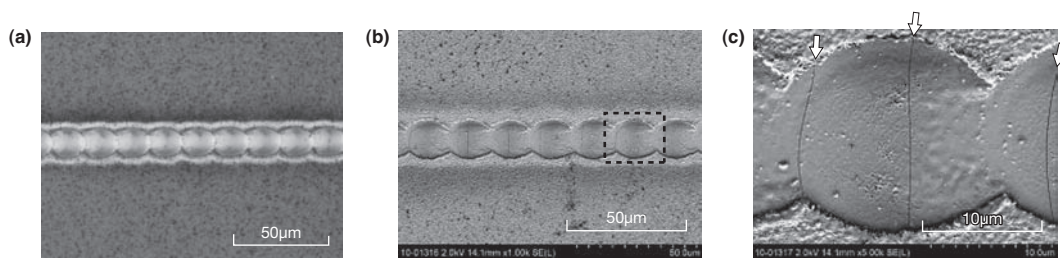


**Photo 1.** P1 structuring on Sample (1) with 200ps-pulses observed with (a) optical micro-scope, (b) SEM, and (c) the enlargement of the area surrounded by broken lines in (b). Three arrows denote the cracks on the glass substrate

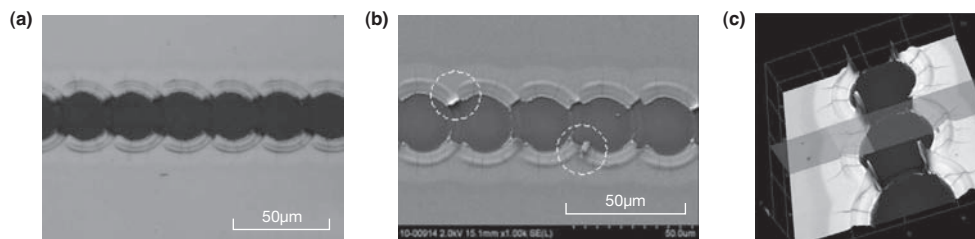


**Photo 2.** P1 structuring on Sample (2) with 20ns-pulses observed with (a) optical micro-scope, (b) SEM, and (c) 3-D analysis with laser microscope. Some rolling up are observed in broken circles in (b)

the risk of the glass damage. In this condition, there has been no cracks, lift-off, debris, or glass damages in P1 structuring on Sample (2) as shown in **Fig. 8**. This result looks as excellent as those processed with 10ps-pulses<sup>(6),(7)</sup>, which suggests that several-hundred-ps pulses may be short enough to structure P1 on CIS solar cells. Moreover, the repetition rate of SumiLas, which is flexible, enables the scanning speed of as high as 5000mm/s. According to the cross-section shown in **Fig. 8 (d)**, the total thickness of the

Mo-film is about 400nm, and that of the residual layer is thinner than 60nm. Namely, the Mo-coating on Sample (2) seems to be composed of 2 layers, namely the first layer is necessary to achieve a good adhesion while the second layer leads to a good conductivity<sup>(13)</sup>.

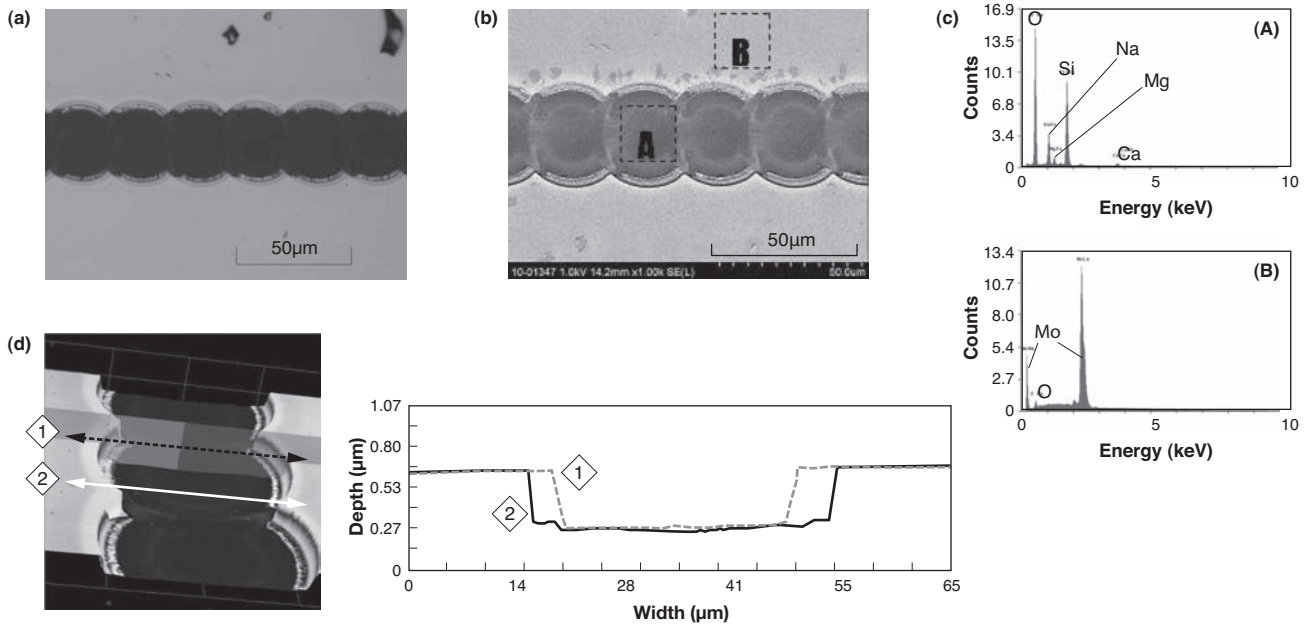


Fig. 8. P1 structuring on Sample (2) with 500ps-pulses observed with (a) optical micro-scope, (b) SEM, (c) EDX, and (d) 3-D analysis with laser microscope

#### 4. Surface Texturing of Stainless Steel<sup>(11),(12)</sup>

As explained in the previous section, the feature of the MOPA type is the flexible repetition rate in comparison to Q-switch lasers or mode-locked lasers. Combining this feature and the high-speed beam scanning devices, such as Galvano scanners, the micro-processing may be available not only on lines but also over areas. One of the laser processing over a certain area is the surface texturing that controls various surface characteristics such as hardness, corrosion resistance and water repellency.

This paper presents the surface texturing of special steel, STAVAX<sup>\*10</sup> manufactured by UDDEHOLM. Both the standard mode and short-pulse mode have been tried for this experiment. Namely, pulse width has been set to 10ns and 0.7ns. Other conditions are shown in **Table 2**. The output beam diameter from SumiLas was set to 1.6mm, and was magnified 5 times by the beam expander. After that, the output beam is inputted into Galvano scanner equipped with the f-theta lens whose focusing length is 100mm. As a result, the beam spot diameter on the work piece has been calculated to be 25µm. The beam scanning speed has been set to 2500mm/s so as to adjust the overlap between adjacent spots to be 0%. As assist gas, nitrogen or compressed air was supplied from the both sides of the workpiece at the pressure of 100kPa.

In order to achieve uniform condition of the surface

before laser radiation, the surface roughness has been adjusted to 0.25µm Ra by grinding.

In the case of 10ns-pulse, uniform periodic pattern can be observed on the surface instead of the grinding mark after scanning 10 times as shown in **Photo 3**. Scanning 100

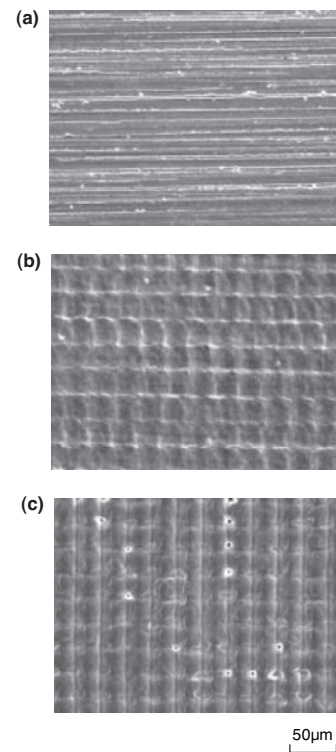


Photo 3. SEM photographs of STAVAX surface with 10ns-pulses, (a) before laser radiation, (b) after 10 times scanning, and (c) after 100 times scanning

Table 2. Surface texturing conditions

| Pulse width (ns) | Average power (W) | Repetition rate (kHz) | Scanning speed (mm/s) |
|------------------|-------------------|-----------------------|-----------------------|
| 10               | 5                 | 100                   | 2500                  |
| 0.7              | 3.5               | 100                   | 2500                  |

times drills several deep holes on the surface. On the other hand, the contact angle of water is almost independent from the scanning number, and seems to be dominantly determined by the kinds of the assist gas, namely nitrogen, compressed air and air, as shown in Fig. 9. The 10ns-pulse

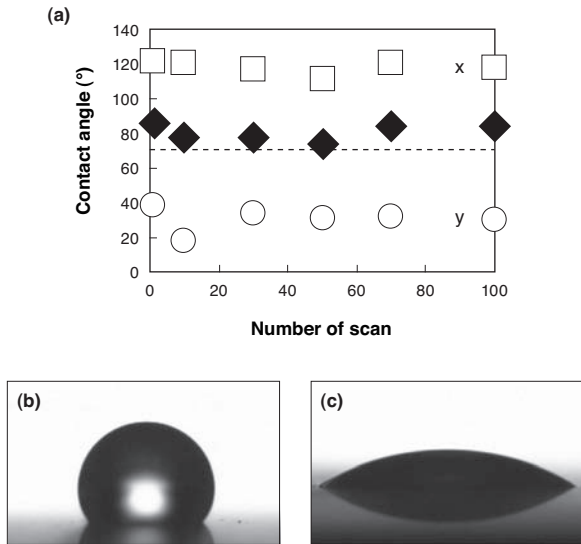


Fig. 9. (a) Relation between contact angle of water and scan number when assist gas is compressed air (square) and nitrogen (filled diamond), and in the air (circle). (b) Water drop at X point and (c) that at Y point in (a)

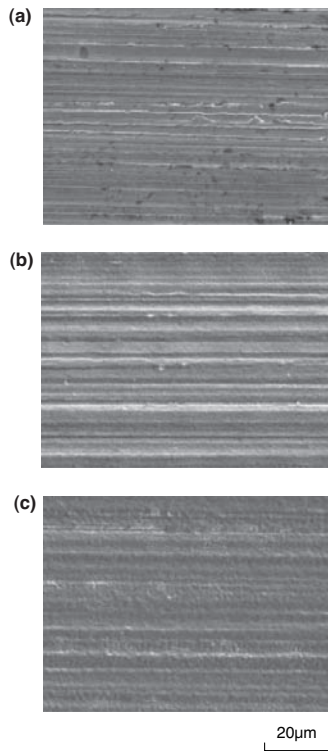


Photo 4. SEM photographs of STAVAX surface with 0.7ns-pulses, (a) before laser radiation, (b) after 10 times scanning, and (c) after 100 times scanning

radiation in air causes excellent wettability.

In the case of 0.7ns-pulse, the surface roughness remains 0.25µm Ra even after scanning 100 times as shown in Photo 4. Nevertheless, the water repellency seems to be controlled both by the scanning number and the assist gas as shown in Fig. 10. Namely, the short pulse mode might enable the control of the water repellency without modifying the surface texture.

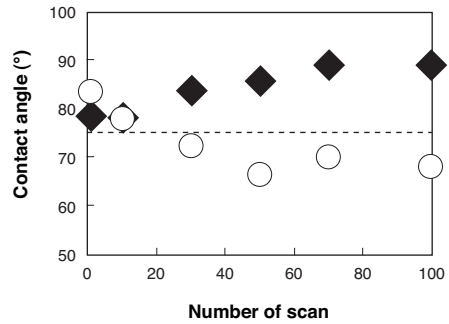


Fig. 10. Relation between contact angle of water and scan number when assist gas is nitrogen (filled diamond), and in the air (circle)

## 5. Wavelength Conversion

Some materials need to be processed at the wavelength shorter than 1060nm. For example, P2 structuring of thin-film solar cells requires the laser beam at 530nm in

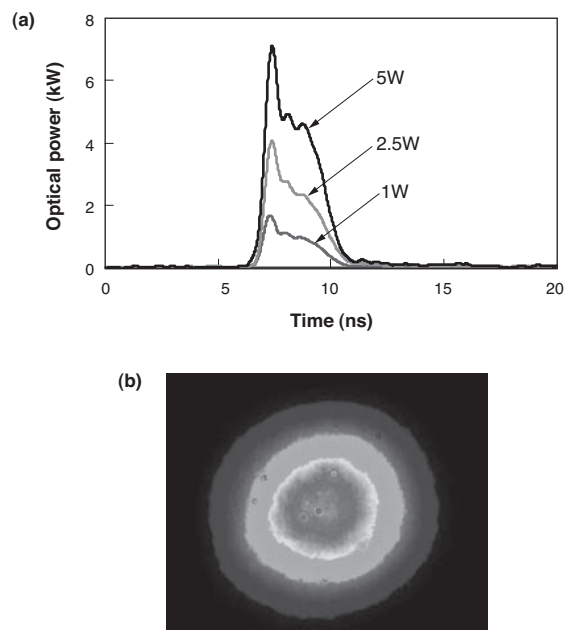


Fig. 11. (a) Output pulse shapes when the average output power is set to 1, 2.5, 5W and the repetition rate to 300kHz and (b) beam profile

order to leave the conduction layer undamaged and to ablate only the absorption layer.

SumiLas has the option to operate at 530nm by inserting the nonlinear crystal in the optical head. Fig. 11 shows the output pulse shapes and the beam profile when the average output power is 5W. We are currently working to increase the output power and tenability of the pulse width.

## 6. Summary

A MOPA-type pulsed fiber laser "SumiLas" with the pulse width tunable from 100ps to 20ns has been developed utilizing optical fiber communication technology such as high-speed pulse modulation, low noise and high gain optical amplification. The short pulse mode operation leads to the drastically different results from that of the standard mode in the applications of P1 structuring and surface texturing on thin-film solar cells. It should be noted that the ns-pulses in the standard mode are preferable for the ablation of TCO coating. In the recent market, there are so many kinds of composite materials containing metal, plastic, glass, ceramics and so on, and therefore, the optimization of laser processing often requires significant time and effort. SumiLas with wide tunable pulse width is a promising tool in this field.

### Technical Term

- \*1 SumiLas is a trademark of Sumitomo Electric Industries, Ltd.
- \*2 Q-switching: Q-value is the ratio of the energy stored during one period to that dissipated during one period. The laser cavity becomes more stable for larger Q-value. Q-switching configuration is a pulse generation method by inserting an optical switch in the laser cavity and modulating the Q-value.
- \*3 Mode-lock: A pulse generation method by adjusting the phase of a plurality of periodically located longitudinal modes. This method is very often used for the ultra-short pulse generation ranging from ps to fs.
- \*4 MOPA: Abbreviation of Master Oscillator Power Amplifier. The output of the master oscillator is amplified by the optical amplifiers in this scheme.
- \*5 CIS: A kind of the novel thin-film solar cell. CIS is the abbreviation of copper, indium, and selenium. There is such a wide variety of the composition that the CIS scheme can be optimized both for low-cost types and for high-end types.
- \*6  $M^2$ : An index of the beam quality.  $M^2$  increases when higher-order modes are included in the beam. For an ideal diffraction-limited beam,  $M^2$  becomes 1.
- \*7 SEM: Abbreviation of scanning electron microscope.
- \*8 EDX: Abbreviation of energy dispersive x-ray spectroscopy. A popular tool for the elementary analysis.
- \*9 New View is a trademark or registered trademark of Zygo Corporation.
- \*10 STAVAX is a trademark or registered trademark of UDDEHOLMSAKTIEBO LAG.

### References

- (1) S. Maruo, I. Miyamoto, ed., "Laser Micro-Processing," Chap. 3, p. 399, Japan Laser Processing Society, Aug 1988
- (2) K. Zhang, A. A. Milner, I. S. Averbukh, Y. Prior, F. Korte, and C. Fallnich, "Femto-second laser material processing," in Proc. of PhAST2005, PThB1, 2005,
- (3) D. Breiting, A. Ruf, and F. Dausinger, "Fundamental aspects in machining of metals with short and ultra short laser pulses," in Proc. of SPIE 5339, pp. 49-63, 2004
- (4) A. Yariv, Quatum Electronics, 3rd Ed., Chapter 20, 1987
- (5) S-P. Chen, H-W. Chem, J. How, and Z-J. Liu, "100W all fiber picosecond MOPA laser," Opt. Express vol. 17, no. 26, pp. 24008-24012, 2009
- (6) H. P. Huber, M. Englmaier, C. Hellwig, A. Heisis, T. Kuznicki, M. Kemnitzer, H. Vogt, R. Brenning, and J. Palm, "High-speed structuring of CIS thin-film solar cells with picosecond laser ablation," in Proc of SPIE vol. 7203, 72030R-1, 2009
- (7) E. Steiger, M. Scharnagl, M. Kemnitzer, and A. Lusskin, "Optimisation of the structuring processes of Cl(G)S thin-film solar cells with an ultra fast picosecond laser and a special beam shaping," in Proc of ICALEO, paper M1107, 2009
- (8) K. T. Vu, A. Malinowski, D. J. Richardson, F. Ghiringhelli, L. M. B. Hickey, and M. N. Zervas, "Adaptive pulse shape control in a diode-seeded nanosecond fiber MOPA system," Opt. Exp. vol. 14, no. 23, pp. 10996-11001, 2006
- (9) S. T. Hendow, J. Sausa, P. T. Guerreiro, N. Schilling, and J. Rabe, "MOPA pulsed fiber laser with controlled peak power and pulse energy for micro machining of hard materials," in Proc. of ICALEO, paper M209, 2009
- (10) S. Tamaoki, Y. Kaneuchi, M. Kakui, B. Baird, N. Paudel, K.A. Wieland, "Development of wide operational range fiber laser for processing thin film photovoltaic panels," in Proc of ICALEO, paper M1306, 2010
- (11) Y. Tanaka, Y. Okamoto and Y. Uno, "Fundamental Study on Surface Modification of Die Material by High-speed Scanning of Pulsed Fiber Laser," Proceedings of Chugoku-Shikoku Branch Conference of Japan Society for Precision Engineering in Yamaguchi, 115, pp. 29-30, Nov. 2009
- (12) Y. Tanaka, Y. Okamoto and Y. Uno, "Investigation into Control of Surface Integrity for Die Material by High-speed Scanning of Pulsed Fiber Laser," Proceedings of Abrasive Technology Conference 2010, D33, pp. 399-400, Aug. 2010.
- (13) W. Hempel, W. Wischmann, "Aging of Molybdenum back contact and its influence on CIGS solar cells," EU PVSEC, Poster session, 3BV.2.39, Sept. 2010.

---

### Contributors (The lead author is indicated by an asterisk (\*)).

#### M. KAKUI\*

• Manager, Optical Components R&D Department, Optical Communications R&D Laboratories

He has been engaged in the development of optical fiber lasers and amplifiers.



#### S. TAMAOKI

• Optical Components R&D Department, Optical Communications R&D Laboratories

#### Y. KANEUCHI

• Assistant Manager, Optical Components R&D Department, Optical Communications R&D Laboratories

**H. KOHDA**

- Assistant Manager, Optical Components R&D Department, Optical Communications R&D Laboratories

**Y. TANAKA**

- Okayama University Graduate School of Natural Science and Technology

**Y. OKAMOTO**

- Assistant Professor, Okayama University Graduate School of Natural Science and Technology

**Y. UNO**

- Professor, Okayama University Graduate School of Natural Science and Technology

**B. BAIRD**

- Managing Director, Summit Photonics LLC.